J|A|C|S ARTICLES

Published on Web 12/01/2010

Processive Replication of Single DNA Molecules in a Nanopore Catalyzed by phi29 DNA Polymerase

Kate R. Lieberman, Gerald M. Cherf, Michael J. Doody, Felix Olasagasti, Yvette Kolodji, and Mark Akeson*

Department of Biomolecular Engineering, Baskin School of Engineering, MS SOE2, University of California, Santa Cruz, California 95064, United States

Received September 29, 2010; E-mail: makeson@soe.ucsc.edu

Abstract: Coupling nucleic acid processing enzymes to nanoscale pores allows controlled movement of individual DNA or RNA strands that is reported as an ionic current/time series. Hundreds of individual enzyme complexes can be examined in single-file order at high bandwidth and spatial resolution. The bacteriophage phi29 DNA polymerase (phi29 DNAP) is an attractive candidate for this technology, due to its remarkable processivity and high affinity for DNA substrates. Here we show that phi29 DNAP−DNA complexes are stable when captured in an electric field across the α-hemolysin nanopore. DNA substrates were activated for replication at the nanopore orifice by exploiting the 3′−5′ exonuclease activity of wild-type phi29 DNAP to excise a 3′-H terminal residue, yielding a primer strand 3′-OH. In the presence of deoxynucleoside triphosphates, DNA synthesis was initiated, allowing real-time detection of numerous sequential nucleotide additions that was limited only by DNA template length. Translocation of phi29 DNAP along DNA substrates was observed in real time at Ångstrom-scale precision as the template strand was drawn through the nanopore lumen during replication.

Introduction

Single-molecule techniques are now used routinely to study nucleic acids in basic science[1−3] and technology.[4,5] Methods using nanoscale pores (nanopores) are advantageous because they can report the length, structure, and composition of unmodified DNA or RNA molecules that are captured in single-file order.[6−9] Data are typically reported as a time series of ionic current as each DNA strand is driven by an applied electric field across a single pore controlled by a voltage-clamped amplifier. Hundreds to thousands of molecules can be examined at high bandwidth and spatial resolution.

Recently, the properties of DNA or RNA molecules bound to nucleic acid processing enzymes have been analyzed at a nanopore orifice. The complexes studied include those of single-stranded DNA with *Escherichia coli* exonuclease I,[10] RNA with the bacteriophage phi8 ATPase,[11] and primer/template DNA substrates bound to the 3′−5′-exonuclease deficient versions of two A-family DNA polymerases, the Klenow fragment of *E. coli* DNA polymerase (KF(exo-)) and bacteriophage T7 DNA polymerase (T7DNAP(exo-)).[12−16] We have demonstrated that T7DNAP(exo-) could replicate and advance a DNA template held in the α-hemolysin (α-HL) nanopore against an 80 mV applied potential.[17] However, due to the low stability of the T7DNAP(exo-)−DNA complex under load, diminished signal-to-noise ratio at 80 mV potential, and the high turnover rate of the polymerase, it was difficult to detect ionic current steps that reported more than three sequential nucleotide additions during replication.

To overcome these limitations, we are examining other DNA-modifying enzymes whose structural and functional properties might facilitate processive catalysis when positioned at a nanopore orifice. An attractive candidate is the bacteriophage phi29 DNA polymerase (phi29 DNAP). This DNA-dependent DNA replicase from the B family of DNA polymerases contains both 5′−3′ polymerase and 3′−5′ exonuclease functions within a single ∼66.5 kD protein chain (reviewed in refs 18 and 19).

(1) Kapanidis, A. N.; Strick, T. *Trends. Biochem. Sci.* **2009**, *34*, 234–243.
(2) Moffitt, J. R.; Chemla, Y. R.; Smith, S. B.; Bustamante, C. *Annu. Rev. Biochem.* **2008**, *77*, 205–228.
(3) Myong, S.; Ha, T. *Curr. Opin. Struct. Biol.* **2010**, *20*, 121–127.
(4) EidJ.; et al. *Science* **2009**, *323*, 133−138.
(5) Harris, T. D.; et al. *Science* **2008**, *320*, 106−109.
(6) Kasianowicz, J. J.; Brandin, E.; Branton, D.; Deamer, D. W. *Proc. Natl. Acad. Sci. U.S.A.* **1996**, *93*, 13770–13773.
(7) Akeson, M.; Branton, D.; Kasianowicz, J. J.; Brandin, E.; Deamer, D. W. *Biophys. J.* **1999**, *77*, 3227–3233.
(8) Ma, L.; Cockroft, S. L. *ChemBioChem* **2010**, *11*, 25–34.
(9) Meller, A.; Nivon, L.; Brandin, E.; Golovchenko, J.; Branton, D. *Proc. Natl. Acad. Sci. U.S.A.* **2000**, *97*, 1079–1084.
(10) Hornblower, B.; Coombs, A.; Whitaker, R. D.; Kolomeisky, A.; Picone, S. J.; Meller, A.; Akeson, M. *Nat. Methods* **2007**, *4*, 315–317.
(11) Astier, Y.; Kainov, D. E.; Bayley, H.; Tuma, R.; Howorka, S. *ChemPhysChem* **2007**, *8*, 2189–2194.
(12) Benner, S.; Chen, R. J.; Wilson, N. A.; Abu-Shumays, R.; Hurt, N.; Lieberman, K. R.; Deamer, D. W.; Dunbar, W. B.; Akeson, M. *Nat. Nanotechnol.* **2007**, *2*, 718–724.
(13) Cockroft, S. L.; Chu, J.; Amorin, M.; Ghadiri, M. R. *J. Am. Chem. Soc.* **2008**, *130*, 818–820.
(14) Gyarfas, B.; Olasagasti, F.; Benner, S.; Garalde, D.; Lieberman, K. R.; Akeson, M. *ACS Nano* **2009**, *3*, 1457–1466.
(15) Hurt, N.; Wang, H.; Akeson, M.; Lieberman, K. R. *J. Am. Chem. Soc.* **2009**, *131*, 3772–3778.
(16) Wilson, N. A.; Abu-Shumays, R.; Gyarfas, B.; Wang, H.; Lieberman, K. R.; Akeson, M.; Dunbar, W. B. *ACS Nano* **2009**, *3*, 995–1003.
(17) Olasagasti, F.; Lieberman, K. R.; Benner, S.; Cherf, G. M.; Dahl, J. M.; Deamer, D. W.; Akeson, M. *Nat. Nanotechnol.* **2010**, *5*, 798−806.
(18) Blanco, L.; Salas, M. *J. Biol. Chem.* **1996**, *271*, 8509–8512.

Following an initial protein-primed stage that ensures the integrity of the ends of the bacteriophage phi29 linear chromosome,[20] phi29 DNAP transitions to a DNA-primed stage and replicates the entire 19.2 kilobase bacteriophage genome without the need for accessory proteins such as sliding clamps or helicases. This highly processive polymerase can catalyze the replication of at least 70 kilobases of DNA *in vitro* following a single binding event to a DNA-primed substrate.[21]

Crystal structures of phi29 DNAP[22,23] revealed the structural basis of this remarkable processivity. The polymerase domain of phi29 DNAP shares the conserved architecture of palm, fingers, and thumb subdomains that resemble a partially opened right hand. In addition, a 32-amino-acid β-hairpin insert that is unique to protein-primed DNA polymerases, together with the palm and thumb subdomains, encircles the primer-template DNA, suggesting that this structure enhances processivity in a manner similar to that achieved by sliding clamp proteins.[24] This same β-hairpin also forms part of a tunnel that surrounds the downstream template DNA. These features indicate that the β-hairpin insert contributes to both the strong DNA binding and processivity of phi29 DNAP. Consistent with this prediction, deletion of the β-hairpin results in a mutant phi29 DNAP that displays distributive DNA synthesis activity rather than the processive activity of the wild-type enzyme and a markedly diminished binding affinity for primer-template duplex DNA.[25]

Experiments using optical tweezers have shown that phi29 DNAP can advance several hundred nucleotides along a template against applied loads of up to ~37 pN,[26] suggesting that this enzyme could replicate a DNA template held atop the nanopore. Here we show that phi29 DNAP−DNA complexes are 3−4 orders of magnitude more stable than KF(exo-)−DNA complexes when captured in an electric field across the α-HL nanopore. DNA substrates in captured complexes were activated for replication by exploiting the 3′−5′ exonuclease activity of wild-type phi29 DNAP to excise a 3′-H terminal residue, yielding a primer strand 3′-OH. In the presence of deoxynucleoside triphosphates (dNTPs), DNA synthesis was initiated, allowing real time detection of numerous sequential nucleotide additions that was limited only by the length of the DNA template.

Methods

Enzymes and DNA Oligonucleotides. The D355A, E357A exonuclease-deficient KF (100,000 U ml^{-1}; specific activity 20,000 U mg^{-1}) was from New England Biolabs. Wild-type phi29 DNAP (833,000 U ml^{-1}; specific activity 83,000 U mg^{-1}) was from Enzymatics. DNA oligonucleotides were synthesized at Stanford University Protein and Nucleic Acid Facility and purified by denaturing PAGE.

Primer Extension and Excision Assays. A 67 mer, 14 base-pair hairpin DNA substrate labeled with 6-FAM at its 5′ end was self-annealed by incubation at 90 °C for four minutes, followed by rapid cooling in ice water. Reactions were conducted with 1 μM annealed hairpin and 0.75 μM phi 29 DNAP(exo+) in 10 mM K-HEPES, pH 8.0, 0.3 M KCl, 1 mM EDTA, 1 mM DTT with $MgCl_2$ added to 10 mM when indicated, and dNTPs added at the concentrations indicated. Reactions were incubated at room temperature for the indicated times and were terminated by the addition of buffer-saturated phenol. Following extraction and ethanol precipitation, reaction products were dissolved in 7 M urea, 0.1X TBE and resolved by denaturing electrophoresis on gels containing 18% acrylamide:bisacrylamide (19:1), 7 M urea, 1X TBE. Extension products were visualized on a UVP Gel Documentation system using a Sybr Gold filter. Band intensities were quantified using ImageJ software (NIH).

Nanopore Experiments. The nanopore device and insertion of a single α-HL nanopore into a lipid bilayer have been described.[7,12,27] Ionic current flux through the α-HL nanopore was measured using an integrating patch clamp amplifier (Axopatch 200B, Molecular Devices) in voltage clamp mode. Data were sampled using an analog-to-digital converter (Digidata 1440A, Molecular Devices) at 100 kHz in whole-cell configuration and filtered at 5 kHz using a low-pass Bessel filter. For voltage-clamped experiments, current blockades were measured at the voltages specified in each figure (*trans*-positive). Experiments were conducted at 23 ± 0.2 °C in buffer containing 10 mM K-HEPES pH 8.0, 1 mM EDTA, 1 mM DTT, 0.3 or 0.6 M KCl as indicated, and 10 mM $MgCl_2$ where indicated. DNA hairpin substrates were annealed prior to each experiment by heating at 95 °C for 3 min and rapidly cooling in an ice bath to prevent intermolecular hybridization.

Active Voltage Control Experiments. Active voltage control of DNAP−DNA complexes atop the nanopore was achieved using finite state machine (FSM) logic, which was programmed with LabVIEW software (version 8, National Instruments) and implemented on a FPGA system (PCI-7831R, National Instruments), as described previously.[12,16] Details of the FSM logic applied in the experiments shown in Figure 2 and Supporting Information, Figure S2, are given in the figure captions.

Nanopore Data Analysis. Dwell time and amplitudes for KF(exo-)−DNA binary complexes were quantified using software developed in our laboratory that detects and quantifies the dwell time and amplitude of EBS and terminal current steps of capture events.[14] Current blockades for phi29 DNAP complexes were quantified using Clampfit 10.2 software (Axon Instruments). Dominant I_{EBS} values for phi29 binary and ternary complexes were obtained by using Clampfit software to determine the peaks of all-points amplitude histograms measured for 1 to 5 s windows in the initial segment of capture events.

Results

Relative Stability of phi29 DNAP−DNA Binary Complexes and KF−DNA Binary Complexes. To perform nanopore experiments, a single α-HL nanopore is inserted in a lipid bilayer separating two chambers (termed *cis* and *trans*) containing buffer solution, and a patch-clamp amplifier applies voltage and measures ionic current (Figure 1a). To examine binary complexes formed between phi29 DNAP and DNA, we used a 14 base-pair DNA hairpin substrate (Figure 1b). As demonstrated previously,[12,15] when a KF−DNA binary complex formed with this substrate is captured in the α-HL pore, the resulting ionic current signature is characterized by an initial enzyme bound state (EBS). This occurs when KF resides atop the pore,[12] holding the double-strand/single-strand junction of the DNA substrate within the confines of the polymerase active site

(19) Salas, M.; Blanco, L.; Lázaro, J. M.; de Vega, M. *IUBMB Life* **2008**, *60*, 82–85.
(20) Salas, M. *Annu. Rev. Biochem.* **1991**, *60*, 39–71.
(21) Blanco, L.; Bernad, A.; Lázaro, J. M.; Martín, G.; Garmendia, C.; Salas, M. *J. Biol. Chem.* **1989**, *264*, 8935–8940.
(22) Berman, A. J.; Kamtekar, S.; Goodman, J. L.; Lázaro, J. M.; de Vega, M.; Blanco, L.; Salas, M.; Steitz, T. A. *EMBO J.* **2007**, *26*, 3494–3505.
(23) Kamtekar, S.; Berman, A. J.; Wang, J.; Lázaro, J. M.; de Vega, M.; Blanco, L.; Salas, M.; Steitz, T. A. *Mol. Cell* **2004**, *16*, 609–618.
(24) Johnson, A.; O'Donnell, M. *Annu. Rev. Biochem.* **2005**, *74*, 283–315.
(25) Rodríguez, I.; Lázaro, J. M.; Blanco, L.; Kamtekar, S.; Berman, A. J.; Wang, J.; Steitz, T. A.; Salas, M.; de Vega, M. *Proc. Natl. Acad. Sci. U.S.A.* **2005**, *102*, 6407–6412.
(26) Ibarra, B.; Chemla, Y. R.; Plyasunov, S.; Smith, S. B.; Lázaro, J. M.; Salas, M.; Bustamante, C. *EMBO J.* **2009**, *28*, 2794–2802.
(27) Vercoutere, W.; Winters-Hilt, S.; Olsen, H.; Deamer, D.; Haussler, D.; Akeson, M. *Nat. Biotechnol.* **2001**, *19*, 248–252.

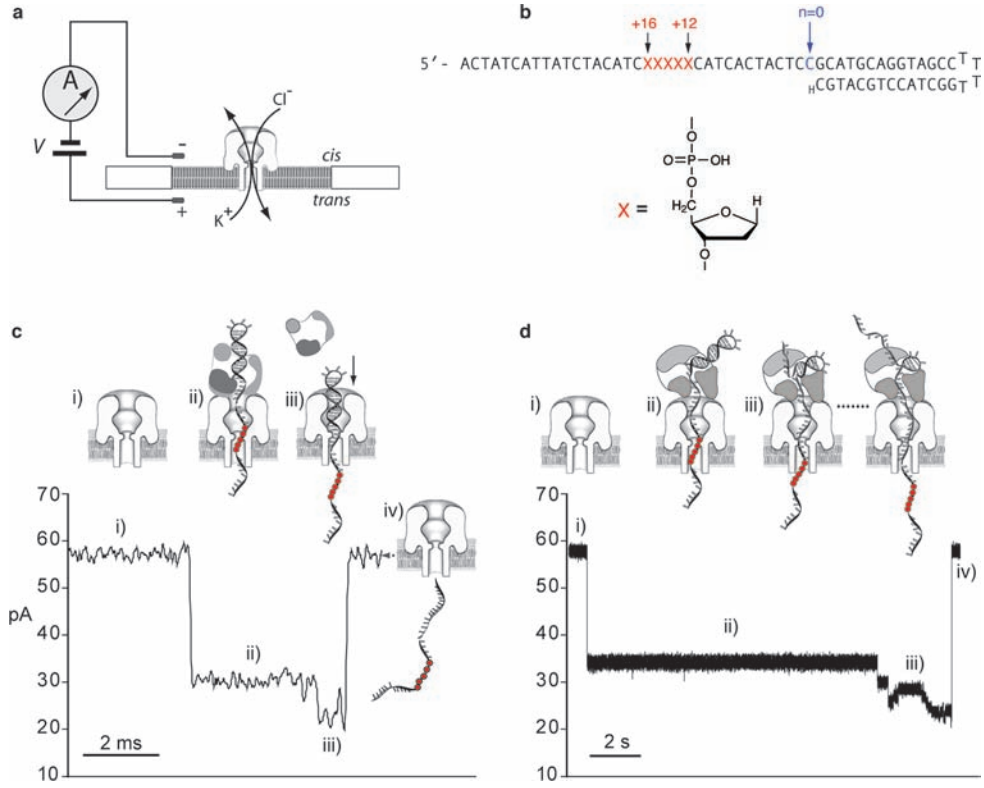

Figure 1. Capture of polymerase−DNA binary complexes in the α-HL nanopore. (a) Schematic of the nanopore device. A single α-HL nanopore is inserted in a 30 μm-diameter lipid bilayer that separates two 100 μL wells containing 10 mM K-HEPES, pH 8.0, 300 mM KCl, 1 mM DTT, and 1 mM EDTA at 23 °C. The nanopore buffer contained no added $MgCl_2$. A membrane potential across the bilayer is determined by AgCl electrodes in series with an Axon 200B amplifier. (b) DNA hairpin substrate used in this experiment. The DNA strand is designed to fold back onto itself forming a 14 bp duplex stem joined by a four-dTMP-residue loop. The 3′ residue of the primer strand is ddCMP. The red X's indicate the five abasic (1′,2′-H) residues that span positions +12 to +16 of the DNA template strand (indicated by numbered arrows above the sequence). Template strand numbering is relative to the first unpaired residue (dCMP) at position $n = 0$ (indicated in blue). The chemical structure of an abasic monomer is shown below the DNA sequence. (c) Ionic current signature for capture of a KF(exo-)−DNA complex at 180 mV applied potential. (i) The open channel current; (ii) enzyme-bound-state current (I_{EBS}); (iii) current caused when voltage-promoted dissociation of KF(exo-) from the DNA causes the duplex segment of the hairpin to drop into the pore vestibule; (iv) return to open channel current caused by unzipping of the DNA hairpin while it is within the nanopore vestibule followed by electrophoresis to the *trans* compartment. Median EBS dwell time for the KF(exo-) binary complexes was 1.9 ms ($n = 199$), identical to the dwell time for binary complexes formed with the same hairpin substrate in the presence of 5 mM $MgCl_2$.[15] (d) Ionic current signature upon capture of a phi29 DNAP−DNA complex at 180 mV potential. (i) The open channel current; (ii) I_{EBS} for the phi29 DNAP−DNA binary complex; (iii) terminal cascade of the current caused by putative unzipping of the DNA duplex while it is bound to phi29 DNAP, and the consequent ratcheting of the DNA through the pore; and (iv) restoration of the open channel current following electrophoresis of the unzipped DNA to the *trans* compartment. The concentrations of KF(exo-) in panel c and phi29 DNAP in panel d were 0.75 μM; in both panels the DNA concentration was 1.0 μM. Note the difference in time scale between panels c and d.

(Figure 1c, ii). In this KF-bound state, the DNA template strand is suspended through the nanopore lumen, which is wide enough to accommodate single-stranded but not duplex DNA. The amplitude of this state (I_{EBS}) can be selectively augmented by an insert of abasic (1′,2′-H) residues within the template strand positioned so that it resides in the nanopore lumen when the polymerase−DNA complex is perched atop the pore,[14,17] such as the 5 abasic residues between template positions +12 to +16 in the DNA hairpin shown in Figure 1b. For KF−DNA binary complexes, the EBS typically lasts a few milliseconds at 180 mV applied potential (Figure 1c, ii). It is followed by a shorter lower amplitude state (Figure 1c, iii), which occurs when the force pulling on the template strand causes dissociation of KF from the DNA, and the duplex DNA drops into the nanopore vestibule. When this occurs the abasic block that was positioned in the pore lumen during the EBS is displaced to the *trans* side of the pore, where it has negligible effect on the amplitude of this terminal current step (~ 20 pA at 180 mV). Unzipping of the DNA hairpin within the vestibule followed by electrophoresis of the strand to the *trans* compartment restores the open channel current (Figure 1c, iv).

Binary complexes between phi29 DNAP and DNA substrates can be formed in the absence of the divalent cations required for both 5′-3′ polymerase and 3′−5′ exonuclease activity.[28] When phi29 DNAP−DNA binary complexes were formed with the hairpin substrate in Figure 1b and captured in the α-HL pore at 180 mV (Figure 1d, ii), the ~35 pA I_{EBS} typically lasted tens of seconds (median =17.6 s, IQR = 25.6, $n = 62$). This is approximately 10,000 times longer than KF−DNA binary complexes under the same conditions (median =1.9 ms, IQR = 2.4 ms, $n = 199$). In contrast to capture events for KF−DNA complexes, these phi29 DNAP−DNA events did not end in a single terminal step, but instead ended in a series of discrete ionic current steps (Figure 1d, iii) that we termed a "terminal cascade". The 3′−5′ exonuclease of wild type phi29 DNAP is inhibited under the conditions of the experiment (1 mM EDTA, absent added Mg^{2+})[29] and thus these current steps are not due to digestion of the primer strand. Therefore we reasoned that the DNA duplex may be unzipping while bound within the

(28) Blasco, M. A.; Lázaro, J. M.; Blanco, L.; Salas, M. *J. Biol. Chem.* **1993**, *268*, 16763–16770.
(29) Blanco, L.; Salas, M. *Nucleic Acids Res.* **1985**, *13*, 1239–249.

confines of the enzyme (Figure 1d, iii). In this scenario, as the template threads out of the complex under tension, the abasic block is drawn out of the lumen in single nucleotide increments that give rise to the sequence of discrete amplitude steps in the terminal cascade (Figure 1d, iii).

This model suggests that the interaction between phi29 DNAP and the DNA is strong enough that the DNA secondary structure unzips due to the force pulling on the template strand before the bond between phi29 DNAP and DNA can be broken. It furthermore predicts that reducing the applied voltage during the terminal cascade could allow the DNA duplex to reanneal within the confines of the enzyme and thus reset the phi29 DNAP−DNA complex to its original position on the DNA template strand, indicated by a return to the ∼35 pA state. To test this prediction, we compared the ability of complexes captured in the presence or absence of Mg^{2+} to recover their original EBS amplitude at 180 mV following a controlled voltage drop. A prerequisite for this comparison is a means to ensure that DNA molecules captured in the presence of Mg^{2+} are intact, so that the nanopore assay compares their fate only after capture. Thus exonucleolytic cleavage of the primer strand in the bulk phase must be miminized during the course of the experiment.

We tested whether a 3′-H terminus on the DNA substrate inhibited the rate of 3′−5′ exonucleolytic cleavage by phi29 DNAP, in a gel assay comparing degradation of two 67 mer 5′-6-FAM labeled hairpin substrates (Figure 2a) bearing either a dCMP (lanes 1−6) or ddCMP (lanes 7−12) terminus. Consistent with the requirement for divalent cations for phi29 DNAP 3′-5′ exonuclease function,[29] no cleavage of either DNA substrate was observed after 45 min incubation in nanopore buffer containing 1 mM EDTA absent added Mg^{2+} (Figure 2a, lanes 1 and 7). With 10 mM Mg^{2+} present, the extent of DNA digestion for the 3′-H substrate was discernably less than for the 3′-OH substrate. After 10 min, while only 24.5% full-length DNA molecules remained for the dCMP-terminated hairpin, 90.5% of the ddCMP-terminated substrate remained intact (Figure 2a, lanes 4 and 10). After 45 min, 4% of the dCMP-terminated substrate and 45% of the ddCMP-terminated substrate remained intact (Figure 2a, lanes 5 and 11). The protection against excision afforded by a 3′-H terminus is further evidenced by the extent of primer extension in the presence of all four dNTPs. For the 3′-H-terminated substrate, the onset of DNA synthesis requires that the ddCMP residue first be excised. Thus, while with the 3′-OH-terminated hairpin >80% of the molecules were extended to the full-length 102 mer product in 45 min (Figure 2a, lane 6), with the 3′-H-terminated hairpin, 79.8% of the DNA substrate remained intact, with only 20.1% full-length extension product (Figure 2a, lane 12). Thus 3′-H-terminated DNA substrates afforded a window following the addition of Mg^{2+} during which phi29 DNAP−DNA complexes could be captured with the DNA substrate intact. We therefore used the ddCMP-terminated hairpin shown in Figure 1b in a nanopore experiment designed to assess the potential for hairpin refolding following initiation of the phi29 DNAP terminal cascade.

In this experiment, upon capture of a phi29 DNAP−DNA complex at 180 mV, a finite state machine (FSM, see Methods) monitored ionic current in real time until the downward current steps of the terminal cascade were detected (Figure 2b, ii). When the ionic current dropped below 31 pA for at least 0.5 ms (red arrow in Figure 2b), the FSM reduced the applied potential to 70 mV (Figure 2b, iii). After two seconds at 70 mV, the applied potential was restored to 180 mV and the amplitude of the phi29 DNAP−DNA complex was remeasured. In the absence of Mg^{2+}, the I_{EBS} level was reproducibly reset to the original 35 pA level in each of 11 molecules tested. This EBS amplitude is indicative of the initial state in which phi29 DNAP is bound to the base-paired duplex with the $n = 0$ template residue positioned in the polymerase active site (Figure 2b, iv), and is consistent with reannealing of the DNA template with an intact primer strand. Importantly, the dominant amplitude during the 70 mV intervals was ∼10.2 pA, with occasional deflections to ∼8.5 pA, measurably above the 6.8 pA value determined for unbound DNA at 70 mV in a control experiment (Figure S2, SI). This indicates that the phi29 DNAP complex remained atop the nanopore orifice without dissociating throughout the lower voltage interval, consistent with a model in which hairpin unzipping at 180 mV and refolding at 70 mV occurs within the confines of the enzyme complex atop the pore.

When the refolding experiment was performed in the presence of 10 mM Mg^{2+}, 16 complexes out of 24 captured in the first 12.5 min after the addition of Mg^{2+} had the ∼35 pA I_{EBS} level, indicating they were formed with intact DNA substrate molecules (Figure 2c, i). This 35 pA state was maintained for several seconds (median = 10.2 s, IQR = 12.7 s, $n = 16$), before ending with a drop in amplitude (Figure 2c, ii). The features of the steps that occurred following the 35 pA state differed from those that characterized the terminal cascade in the absence of Mg^{2+} (compare Figure 2b, ii to 2c, ii). For these complexes, when the voltage was reduced to 70 mV for two seconds and then restored to 180 mV, the 35 pA I_{EBS} level did not reset for any of the complexes tested (Figure 2c). This is in contrast to the phi29 DNAP−DNA complexes captured in the absence of Mg^{2+}, and it indicates that the DNA substrates, which had been captured intact, were modified by exonucleolytic cleavage while they were held atop the pore.

Mapping the Effect of Template Abasic Insert Position on I_{EBS} for DNA Substrates Bound to phi29 DNAP. Our strategy for detecting DNA synthesis catalyzed by polymerase−DNA complexes held atop the nanopore employs monitoring changes in ionic current as a block of abasic residues in the template strand is drawn into and through the nanopore lumen in single nucleotide increments when the polymerase advances along the template.[14,17] This approach permits the recognition of sequential Ångstrom-scale movements driven by the enzyme.

As a prelude to DNA replication experiments with phi29 DNAP, we established a reference map that related I_{EBS} to the position of a 5 abasic block within the template strand of DNA hairpin substrates (Figure 3). To construct this map, phi29 DNAP was bound to each of a series of substrates that contained a block of 5 consecutive abasic residues, sequentially displaced by one nucleotide (Figure 3a). We measured the I_{EBS} in buffer containing 0.3 M KCl for captured complexes under two conditions: (i) 1 mM EDTA with no added Mg^{2+}, which permits formation of binary complexes without supporting nucleotide excision or addition (Figure 3b, lane 1); and (ii) 10 mM Mg^{2+}, 400 μM ddCTP, and 100 μM dGTP. These latter conditions maintained the intact status of 98.2 and 96% of 3′-H-terminated hairpin molecules in the bulk phase for 10 and 45 min, respectively (Figure 3b, lanes 6 and 7). Protection was afforded by ddCTP, which permitted the polymerase function of phi29 DNAP to restore the ddCMP terminus of molecules if it was excised by the exonuclease function (Figure 3b, lanes 3 and 4). Protection was enhanced by the presence of dGTP, which is complementary to the template residue at $n = 0$ and can form a phi29 DNAP−DNA−dGTP ternary complex in the presence

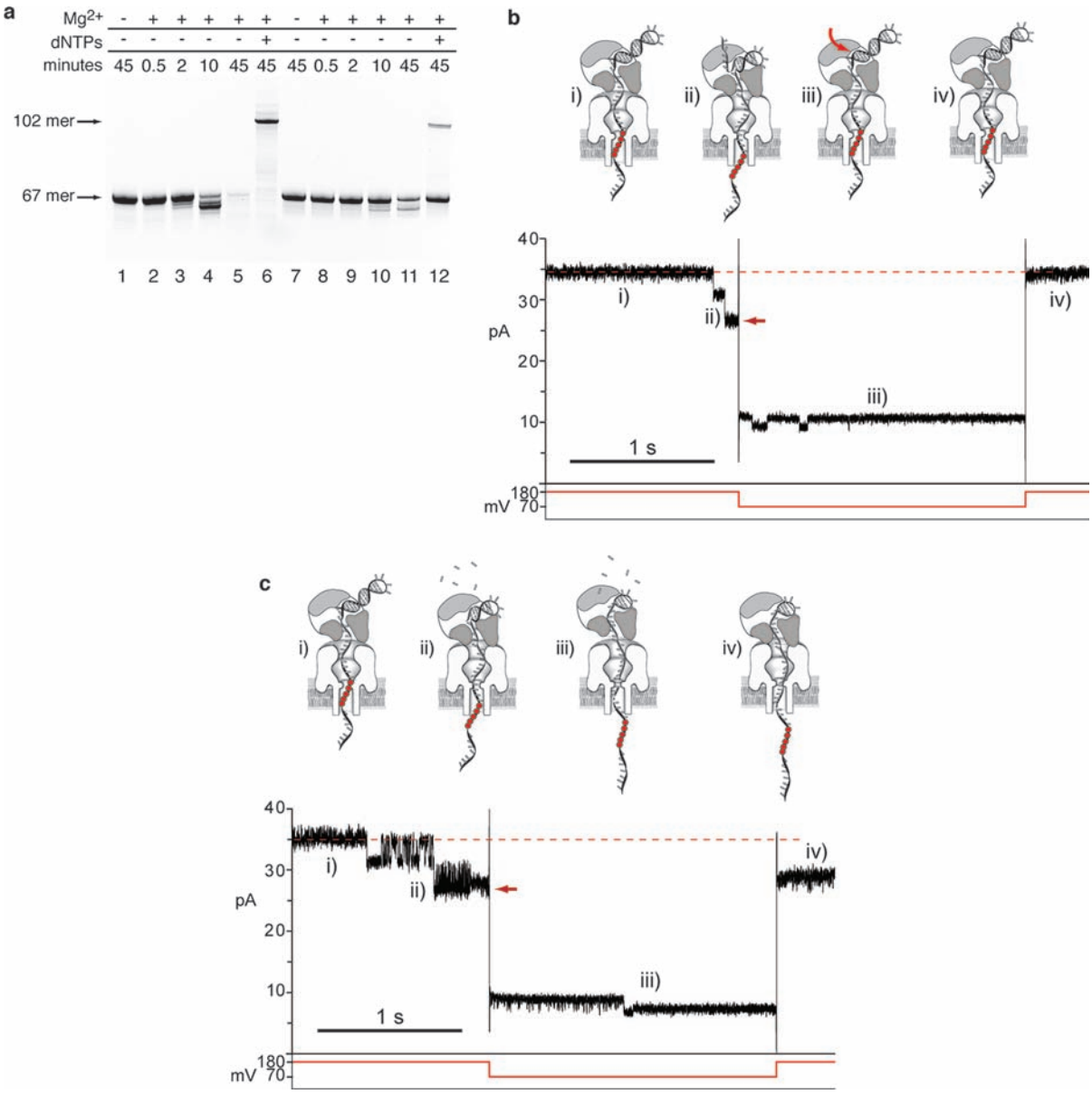

Figure 2. Duplex unzipping during DNA hairpin dissociation from phi29 DNAP at 180 mV applied potential is reversed at 70 mV. (a) Protection in the bulk phase of a 14 bp DNA hairpin substrate from phi29 DNAP-catalyzed 3′−5′ exonucleolytic degradation by a ddNMP (3′-H)-terminated primer strand. Hairpin substrates (1 μM) labeled with 5′-6-FAM bearing either a 3′-OH (lanes 1−6) or 3′-H (lanes 7−12) terminus were incubated at room temperature with 0.75 μM phi29 DNAP in buffer containing 10 mM K-HEPES, pH 8.0, 300 mM KCl, 1 mM DTT, and 1 mM EDTA for the times indicated. The reactions in lanes 1 and 7 contained no added $MgCl_2$; those in lanes 2−6 and 8−12 contained 10 mM $MgCl_2$. The reactions in lanes 6 and 12 also contained 200 μM each dATP, dCTP, dGTP, and dTTP. Reaction products were resolved on an 18% denaturing polyacrylamide gel. Positions of the gel bands corresponding to the intact 67-mer starting substrates and the 102-mer full-length extension products are indicated with arrows on the side of the gel. Sequences of the 5′-6-FAM-labeled DNA hairpins are shown in Figure S1 (Supporting Information, SI). (b) Steps in the pathway of voltage-promoted phi29 DNAP−DNA complex dissociation are reversible. In this experiment, the buffer contained 1 mM EDTA and no added $MgCl_2$ in order to prevent phi29 DNAP 3′−5′ exonucleolytic activity. (i) Capture of a phi29 DNAP−DNA binary complex formed with the hairpin substrate shown in Figure 1b. This positions the abasic insert, located between positions +12 to +16 of the template strand, in the limiting aperture of the nanopore lumen, yielding an I_{EBS} of 35 pA; (ii) after several seconds in this 35 pA state, a stepwise reduction in current through the nanopore ensues, as the 180 mV applied potential promotes unzipping of the DNA duplex and progressive movement of the five abasic block-out of the limiting aperture; (iii) when the current amplitude dropped below 31 pA for at least 0.5 ms, a finite state machine (FSM) reduced the voltage to 70 mV (red arrow in the current trace) for 2 s to allow reannealing of the DNA duplex to its original state (indicated by the curved red arrow in the cartoon) while retaining the phi29 DNAP−DNA complex on the α-HL nanopore; (iv) after 2 s at 70 mV, the FSM restored the applied potential to 180 mV. Recovery of the original 35 pA current level (dashed red line) indicates that the phi29 DNAP−DNA complex has reset to its original captured state. (c) phi29 DNAP−DNA complex dissociation under conditions that permit 3′−5′ exonucleolytic excision of nucleotides from the DNA primer strand. In this experiment, 10 mM $MgCl_2$ was added to the buffer described in panel b. (i) Capture of a phi29 DNAP−DNA complex in the α-HL nanopore positions the 5 abasic block in the limiting aperture of the nanopore lumen, yielding an I_{EBS} of 35 pA that is diagnostic for a complex bearing a DNA substrate with an intact ddCMP terminus; (ii) movement of the 5 abasic block-out of the limiting aperture results in a reduction in current through the nanopore, which can be caused by (1) unzipping of the DNA duplex or (2) phi29 DNAP-catalyzed 3′−5′ exonucleolytic degradation of the primer strand while the complex is retained atop the pore; (iii) as in panel b(iii), when the current amplitude dropped below 31 pA for at least 0.5 ms, the FSM reduced the voltage to 70 mV for 2 s to allow for reannealing of the DNA duplex (red arrow in the current trace), while retaining the phi29 DNAP−DNA complex on the nanopore; (iv) in contrast to panel b(iv), restoration of 180 mV applied potential after 2 s by the FSM does not recover the original 35 pA I_{EBS} (dashed red line), indicating that, under conditions that permit catalysis of 3′−5′ exonucleolytic excision in phi29 DNAP−DNA complexes atop the pore, the original captured state is not recovered.

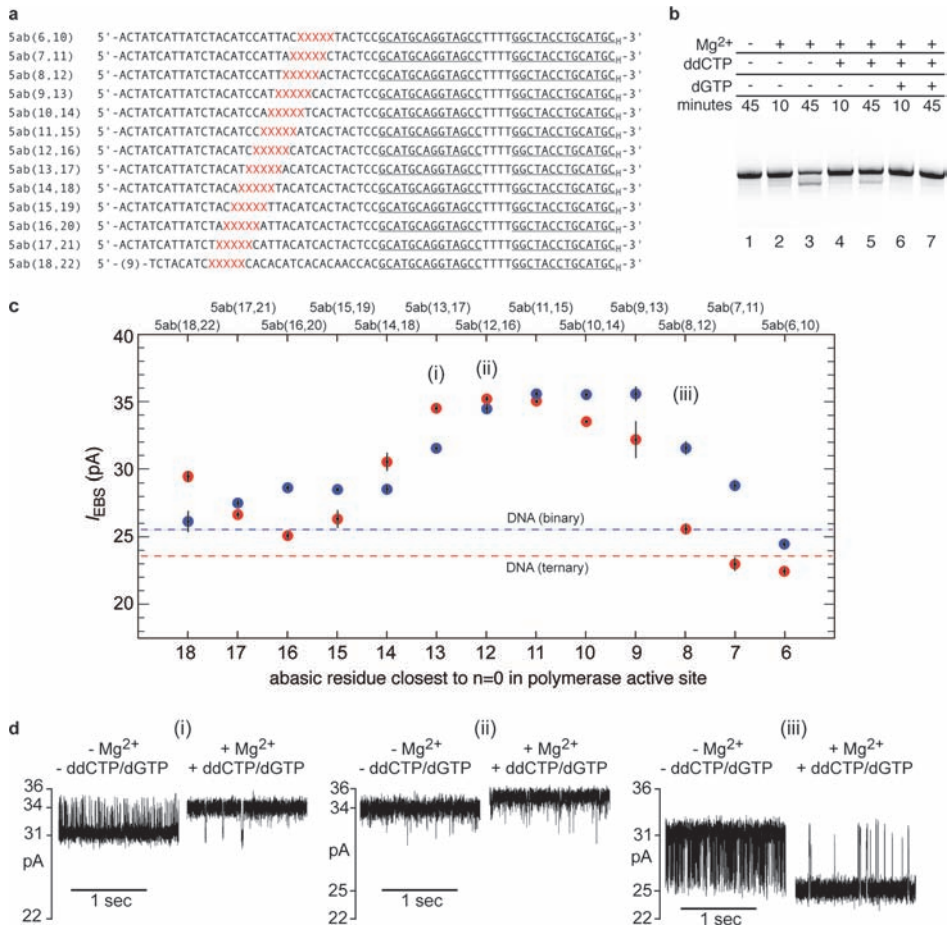

Figure 3. EBS amplitudes at 180 mV of phi29 DNAP−DNA complexes as a function of abasic insert position in DNA template strands. (a) DNA hairpins used in phi29 DNAP mapping experiments. In each sequence, red X's indicate the positions of the abasic (1′,2′-H) residues. Abasic configuration is denoted as 5ab(*x*,*y*), where 5 is the number of abasic residues in the insert, and *x* and *y* respectively indicate the distance (in nucleotides) of the first and last abasic residues of the insert, measured from the template strand dNMP at $n = 0$ in the polymerase catalytic site. The self-complementary sequence blocks that form the 14-base-pair hairpin are underlined. The abasic configuration for each hairpin is indicated to the left of each sequence. (b) State of hairpin substrates in the bulk phase during nanopore experiments to map the amplitude of phi29 DNAP−DNA complexes. A 5′-6-FAM, 3′-H 14 bp hairpin (1 μM) was incubated at room temperature with 0.75 μM phi29 DNAP in buffer containing 1 mM EDTA, absent (lane 1) or present (lanes 2−7) 10 mM $MgCl_2$ for the times indicated. Reactions included 400 μM ddCTP (lanes 4 and 5) or 400 μM ddCTP and 100 μM dGTP (lanes 6 and 7). The conditions in lane 1 are those employed to map the amplitude of the phi29 DNAP−DNA binary complexes. Conditions in lanes 6 and 7 are those used to map the amplitude of phi29 DNAP−DNA−dGTP ternary complexes. (c) Map of dominant amplitude values in buffer containing 0.3 M KCl for the EBS of phi29 DNAP−DNA binary (blue circles) or phi29 DNAP−DNA−dGTP ternary (red circles) complexes. Each point represents the average I_{EBS} determined from three separate experiments ± the standard error. The blue and red dashed lines indicate the amplitudes for phi29 DNAP binary and ternary complexes, respectively, formed with a DNA hairpin substrate composed of normal DNA residues bearing no abasic insert. (d) Current traces showing representative segments of events for complexes captured under binary (labeled as -Mg^{2+}, -ddCTP/dGTP) or ternary (labeled as +Mg^{2+}, +ddCTP/dGTP) mapping conditions, formed with DNA hairpin substrates with the abasic configurations (i) 5ab(13,17), (ii) 5ab(12,16), or (iii) 5ab(8,12). The positions on the map for complexes formed with these substrates are indicated by corresponding lower-case Roman numerals in panel c.

of the 3′-H-terminated DNA substrate[22] that can increase the proportion of time the primer terminus resides in the polymerase domain rather than in the exonuclease domain (Figure 3b, lanes 6 and 7; Figure S3, SI). The complex formed in the presence of Mg^{2+}, ddCTP, and dGTP is therefore operationally defined as a *ternary complex* in this study.

The I_{EBS} maps for phi29 DNAP binary complexes (blue dots) and ternary complexes (red dots) are shown in Figure 3c. Both maps were similar to a map determined for KF(exo-)−DNA−dNTP ternary complexes at 80 mV using a six abasic template insert.[17] In 0.3 M KCl at 180 mV, I_{EBS} ranged from 22.3 pA for the ternary complex formed with the 5ab(6,10) substrate (abasic block spanning template positions +6 to +10 measured from $n = 0$ in the polymerase catalytic site), to 35.4 pA for the binary complexes formed with the 5ab(11,15) and 5ab(9,13) substrates (abasic blocks spanning template positions +11 to +15, and +9 to +13, respectively). This gives a dynamic amplitude range of at least 13 pA for the detection of enzyme movements during polymerization or exonucleolytic reactions.

At all positions within the map, I_{EBS} for the binary and ternary complexes were offset from one another. The direction and the scale of the offset depended in part on the position along the map. For example, at position (i) (Figure 3c), the change from a binary complex to a ternary complex caused an I_{EBS} increase from 31.5 pA to 34.5 pA. By comparison, at position (ii) (Figure 3c) the binary to ternary change resulted in a relatively small current increase from 34.4 to 35.2 pA, and at position (iii) (Figure 3c) the binary to ternary transition caused a large I_{EBS} current *decrease* from 31.5 to 25.5 pA. Interestingly, the direction and magnitude of an ionic current flicker within the binary state often predicted the dominant amplitude observed for the ternary complex formed with the same substrate (Figure 3d).

The results of the mapping experiments permit a prediction based upon the model proposed for the molecular events that give rise to the terminal cascade (Figures 1 and 2): the sequence of current steps in the terminal cascade of binary complex capture events should vary in a manner that is dependent on the initial position of the abasic block in the complex. This was found to be the case. For example, when the duplex segment of the 5ab(6,10) substrate was unzipped during the terminal cascade, the abasic block was drawn from its position proximal to the enzyme toward the *trans* chamber. This resulted in a series of current steps with a ~36 pA peak as the abasic block traversed the pore lumen (Figure S4a, SI). In contrast, for binary complexes formed with the 5ab(18,22) substrate, the initial position of the abasic block is distal from the enzyme. When this substrate is unzipped in the terminal cascade, no amplitude peak is observed (Figure S4b, SI).

Controlled Translocation of DNA Templates in the Nanopore Catalyzed by phi29 DNAP. Results from our laboratory have shown that advance of a DNA template in the α-HL nanopore could be detected at single nucleotide precision during replication by T7DNAP(exo-).[17] However, for the majority of complexes with this enzyme only one or two nucleotide addition cycles could be monitored. To determine if phi29 DNAP was more efficient at catalyzing sequential nucleotide additions on the nanopore, we measured phi29 DNAP-driven displacement of synthetic DNA substrates molecules bearing 5 abasic inserts in their template strands. The map in Figure 3 was used to interpret changes in I_{EBS} as single nucleotides were enzymatically added to or removed from the DNA 3′ terminus.

The experiment in Figure 2c showed that the slow excision of a ddNMP residue in the bulk phase could be exploited to capture complexes in the presence of Mg^{2+} in which the primer strand was intact. Importantly, this experiment also showed that excision of the ddNMP residue could be achieved on the pore, exposing the 3′-OH of the −1 residue and thus yielding a substrate that is potentially competent for synthesis reactions atop the pore in the presence of dNTPs. Consistent with previous findings,[30,31] the gel assay in Figure 2a showed that in the presence of dNTPs the polymerization reaction dominated over the exonuclease reaction in bulk phase. These findings were essental to our strategy for DNA replication experiments: capture phi29 DNAP complexes bearing intact 3′-H-terminated substrates in the presence of dNTPs, allow the excision reaction to occur on the pore, and use an abasic block marker in the template strand to determine unambiguously whether the polymerization reaction can be observed for complexes held atop the pore. Using this strategy, the majority of complexes captured in the nanopore should initiate replication at the same template position (−1 relative to the original $n = 0$ position of the starting substrate).

Because dGTP can slow the rate of ddCMP excision due to formation of ternary complexes (Figure 3b, Figure S3, SI) we chose to conduct initial nanopore synthesis experiments using 20 μM each of dATP, dCTP, dTTP and 5 μM dGTP. We determined the effect of these conditions on the state of the DNA substrate molecules in bulk phase in a gel assay using the 5′-6-FAM, 3′-H hairpin substrate (Figure 4b). After 10 min, 82.5% of the 67 mer starting substrate remained intact, and 13.6% was extended to the 102 mer product. After 20 min, these proportions were 69.4% and 26.1% extension product, and by 45 min almost 30% of the fluorescein labeled hairpin had been extended. We therefore confined our measurements in the nanopore experiments to the first 10 min following the addition of Mg^{2+} and dNTP substrates to the *cis* chamber.

In initial nanopore replication experiments under these conditions (Figure 4), we used a DNA substrate with the starting abasic configuration 5ab(15,19) bearing a 3′ ddCMP terminus (Figure 4a). Typical ionic current traces for capture of phi29 DNAP−DNA complexes at 180 mV with this substrate in the presence of 10 mM Mg^{2+}, without or with dNTPs, are shown in Figure 4c and d, respectively. The dominant initial I_{EBS} upon capture was ~29 pA under both conditions, with deflections to ~26 pA consistent with an oscillation between the map values for 5ab(15,19) binary and ternary complexes (Figure 3c). Under both conditions, there was a delay at this starting I_{EBS} level, afforded by the slow excision of the 3′ ddCMP terminus, after which a series of current changes ensued. We interpret the current changes in the experiment conducted in the absence of dNTPs (Figure 4c) as follows: upon ddCMP excision, the phi29 DNAP exonuclease continued to sequentially cleave nucleotides from the primer terminus, resulting in a progressively shorter duplex segment and greater distance between the enzyme and the abasic insert. The abasic segment was thus moved through the pore toward the *trans* compartment, causing a progressive ionic current decrease. Eventually, the ionic current returned to the open channel state, consistent with dissociation of the DNA molecule from phi29 DNAP and its subsequent electrophoresis into the *trans* compartment.

In contrast, when the experiment was conducted in the presence of 20 μM each dATP, dCTP, dTTP, and 5 μM dGTP a different ionic current pattern resulted, characterized by a peak at 35.4 pA (Figure 4d). We hypothesized that these current changes occurred because, following phi29 DNAP excision of the ddCMP residue protecting the DNA 3′ terminus, the presence of dNTPs favored nucleotide additions catalyzed by phi29 DNAP while atop the pore. The duplex DNA segment was lengthened as phi29 DNAP moved progressively closer to the abasic insert within the DNA template, drawing it through the nanopore lumen with the attendant traversal of the major ionic current peak between abasic configurations 5ab(15,19) to 5ab(6,10) in the map in Figure 3c. Several DNA template replication reactions, catalyzed by phi29 DNAP−DNA complexes captured in series during this experiment are shown in Figure 4e.

In the gel experiment shown in Figure 4b, in addition to the starting 67 mer hairpin substrate and the full-length extension products, intermediate bands corresponding to partial extension products accumulated with time (Figure 4b, lanes 6 and 7). These products could arise due to depletion of dNTP pools in the bulk phase, as an increasing fraction of the DNA substrate molecules which are present at 1 μM in both the gel and nanopore assays are replicated. Because this has the potential to affect the extent and rate of synthesis catalyzed by phi29 DNAP complexes atop the pore, we examined whether this could be minimized by using a higher concentration of dNTPs.

We measured the extent of primer extension for the 5′-6-FAM, 3′-H-terminated hairpin in the presence of 100 μM each of dGTP, dCTP, dTTP, and dATP as a function of time (Figure 5a and b). Under these conditions the rate of accumulation of the full-length product was slower than in the experiment in Figure 4b (using 20 μM each of dCTP, dTTP, dATP and 5 μM dGTP), likely due to the more efficient inhibition of excision

(30) Garmendia, C.; Bernad, A.; Esteban, J. A.; Blanco, L.; Salas, M. *J. Biol. Chem.* **1992**, *267*, 2594–2599.
(31) Truniger, V.; Lázaro, J. M.; Esteban, F. J.; Blanco, L.; Salas, M. *Nucleic Acids Res.* **2002**, *30*, 1483–1492.

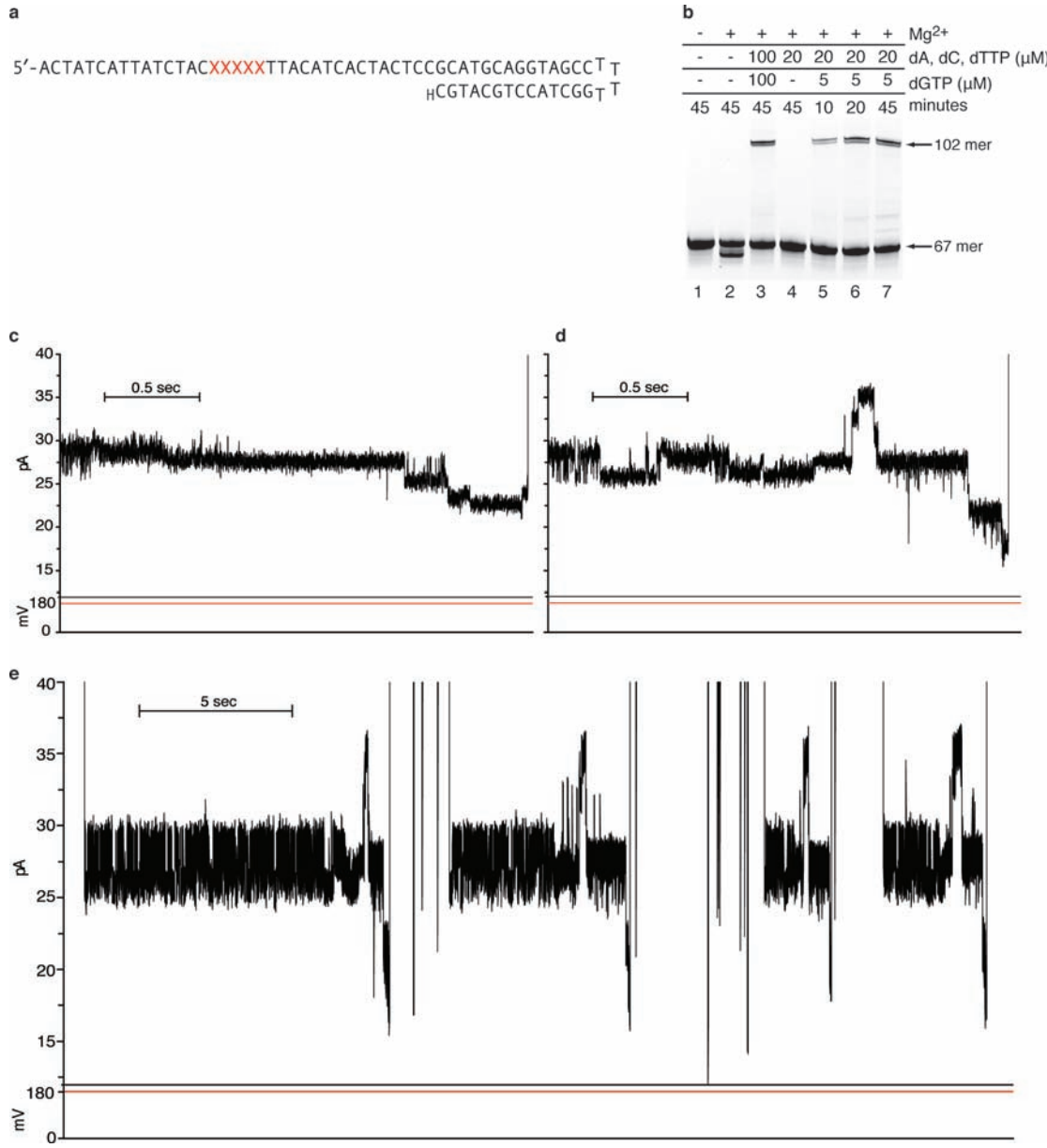

Figure 4. DNA replication catalyzed by phi29 DNAP on the nanopore. (a) DNA hairpin substrate for nanopore replication experiments. The starting abasic configuration for this substrate is 5ab(15,19). The onset of primer extension requires exonucleolytic excision of the terminal ddCMP residue, after which fifteen nucleotides can be added before the enzyme reaches the abasic block. As replication proceeds, the 5 abasic residue block will be drawn through and past abasic configurations 5ab(15,19) to 5ab(6,10), which comprise the major peak in the map in Figure 3. (b) Phi29 DNAP-catalyzed primer extension of a DNA hairpin substrate in bulk phase under nanopore experiment conditions. A 67 mer, 5′-6-FAM, 3′-H 14 bp hairpin (1 μM) was incubated at room temperature for the indicated times with 0.75 μM phi29 DNAP in buffer containing 10 mM K-HEPES, pH 8.0, 0.3 M KCl, 1 mM DTT, and 1 mM EDTA, absent (lane 1) or present (lanes 2−7) 10 mM $MgCl_2$, with dNTPs added as indicated. Reaction products were resolved on an 18% denaturing polyacrylamide gel. Lanes 5−7 show the extent of primer extension at 10, 20, and 45 min in bulk phase under the dNTP substrate conditions of the nanopore experiments in panels d and e (5 μM dGTP, 20 μM each dATP, dCTP, and dTTP). (c) Representative capture event for a phi29 DNAP−DNA complex formed with the 5ab(15,19) hairpin shown in panel a, in the presence of 1 mM EDTA and 11 mM $MgCl_2$, absent dNTPs. (d) Representative capture event for a phi29 DNAP−DNA complex formed with the 5ab(15,19) hairpin shown in panel a in the presence of 1 mM EDTA, 11 mM $MgCl_2$, and 5 μM dGTP, 20 μM each dATP, dCTP, and dTTP. (e) Phi29 DNAP-catalyzed replication of individual DNA substrate molecules captured in series. The current trace is shown in real time; the first event in the series of four is the event shown expanded in panel d. Current traces shown in panels c−e were collected within the first 10 min of the addition of $MgCl_2$ (c) or $MgCl_2$ and dNTPs (d, e) to minimize dNTP depletion due to bulk phase reactions.

of the ddCMP terminus afforded by the higher dGTP concentration. After 20 min, 86.3% of the starting DNA substrate remained intact, and 13.6% was fully extended (Figure 5a, lane 6, and Figure 5b), compared to 69.4% and 26.1% for these species, respectively, in reactions conducted for the same amount of time with the lower concentrations of dNTPs (Figure 4b, lane 6). Importantly, even after 30 min, accumulation of shorter extension products was below the limit of detection of the assay. We therefore used dNTP substrates at a concentration of 100 μM each in subsequent replication experiments.

To test the model proposed for the ionic current signatures observed in the replication experiment in Figure 4d and e, we used a DNA hairpin substrate in which the first template dTMP residue was at a defined position relative to the abasic insert (Figure 5). When DNA synthesis reactions are conducted with this substrate in the presence of 100 μM each of

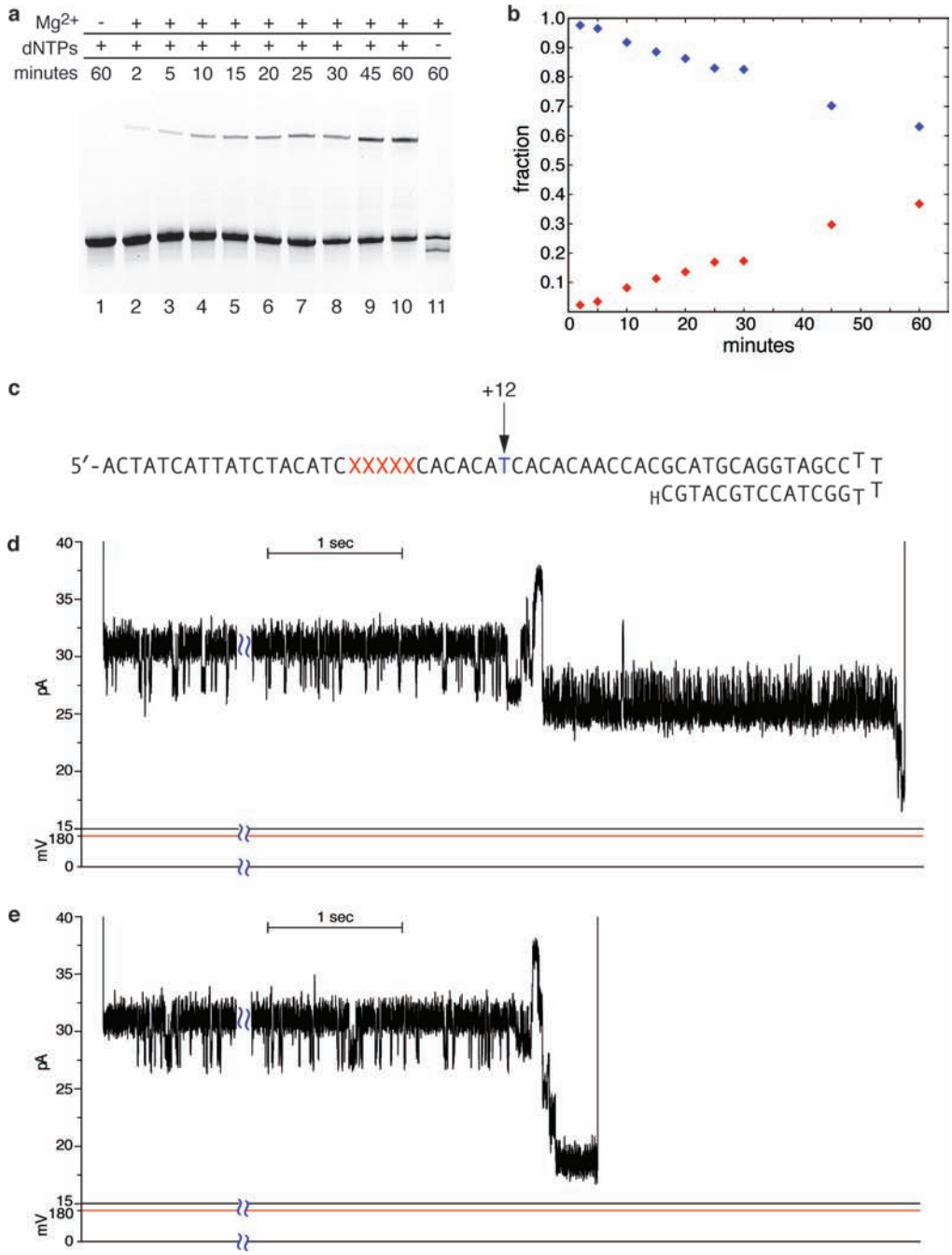

Figure 5. Phi29 DNAP-catalyzed replication up to or through a specific template position. (a) Time course of primer extension for a DNA hairpin substrate in bulk phase, in the presence of phi29 DNAP and 100 μM each dGTP, dCTP, dTTP, and dATP. A 67-mer 5′-6-FAM, 3′-H 14 bp hairpin (1 μM) was incubated at room temperature with 0.75 μM phi29 DNAP in buffer containing 1 mM EDTA, absent (lane 1) or present (lanes 2−7) 10 mM $MgCl_2$ and 100 μM each of all four dNTPs (lanes 1−10) for the times indicated. The onset of primer extension requires exonucleolytic excision of the terminal ddCMP residue preceding processive dNTP additions. Reaction products were resolved on an 18% denaturing polyacrylamide gel. (b) The fluorescence intensity of bands in the gel in panel a corresponding to the intact, unextended hairpin (blue diamonds) and the extension product (red diamonds) were quantified using ImageJ software (NIH). For each lane, the fraction of the total fluorescence for these two bands was plotted as a function of reaction time. (c) DNA hairpin substrate for nanopore replication experiments. The starting abasic configuration is 5ab(18,22). In the presence of dGTP, dCTP, dTTP, and ddATP, 12 nucleotides can be added up to ddATP addition in response to the first template dTMP residue (blue). This dTMP residue is positioned such that reaching this end point requires replication of a segment of template during which the abasic block (red X's) is drawn into and through the nanopore lumen. After ddATP incorporation, a phi29 DNAP−DNA−dTTP ternary complex can be formed with abasic configuration 5ab(6,10). In the presence of dGTP, dCTP, dTTP, and dATP, replication can proceed past the +12 position up to the abasic block. (d) phi29 DNAP-catalyzed replication on the hairpin substrate shown in panel c in the presence of 100 μM each dGTP, dCTP, dTTP, and ddATP, in buffer containing 0.3 M KCl and 10 mM $MgCl_2$. (e) phi29 DNAP-catalyzed replication after 200 μM dATP was added to the experiment shown in panel (d). Events shown in panels d and e are representative of dozens of complexes captured. Events in a control experiment in which 100 μM each dGTP, dCTP, dTTP, and dATP were added absent ddATP were identical to the representative event shown in panel e. Complexes were captured within the first 10 min after the addition of $MgCl_2$ to the nanopore chamber.

dGTP, dCTP, dTTP, and ddATP, 12 nucleotides can be added, during which the abasic block will be drawn from its starting position of 5ab(18,22), across the 35.4 pA peak at 5ab(11,15), to position 5ab(6,10). After reaching the dTMP residue at position +12, replication is predicted to stall. In contrast, replication reactions conducted in the presence of

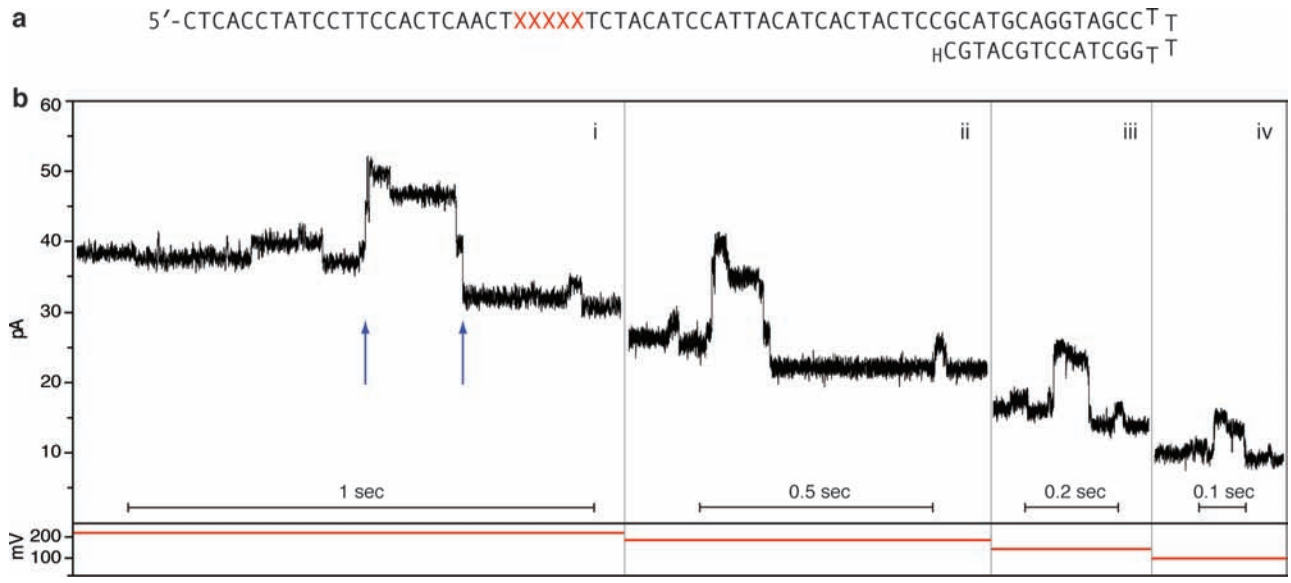

Figure 6. Phi29 DNAP-catalyzed replication by complexes held atop the nanopore at different voltages. (a) DNA hairpin substrate for nanopore replication experiments. The starting abasic configuration for this substrate is 5ab(25,29). After the exonucleolytic excision of the terminal ddCMP residue that is required for initiation of DNA synthesis, 25 nucleotides can be added before the enzyme reaches the abasic block. During DNA synthesis, the 5 abasic insert will be drawn through and past abasic configurations 5ab(18,22) to 5ab(6,10), which spans the positions mapped in Figure 3. (b) Representative current traces showing phi29 DNAP replication of the hairpin substrate shown in panel a, in buffer containing 0.3 M KCl, 10 mM $MgCl_2$, in the presence of 100 μM each dGTP, dCTP, dTTP and dATP. Traces are shown for synthesis at (i) 220 mV, (ii) 180 mV, (iii) 140 mV, and (iv) 100 mV applied potential. Synthesis was examined within the first 10 min after the addition of $MgCl_2$ to the nanopore chamber. The blue arrows below the 220 mV trace indicate the starting and end states used to quantify the synthesis rate at 220 and 100 mV.

100 μM each dGTP, dCTP, dTTP, and dATP should proceed past the +12 position.

When phi29 DNAP complexes formed with this DNA substrate were captured under both of these conditions, an initial period of several seconds occurred during which the dominant current amplitude was ~31 A, with oscillations to ~27 pA (Figure 5d and e), similar to the map values for the ternary and binary complexes for this 5ab(18,22) configuration (Figure 3c). After this state ended, the 35.4 pA ionic current peak was rapidly traversed, indicative of the abasic block being drawn through the lumen. If dGTP, dCTP, dTTP, and ddATP were present in the *cis* chamber, after traversing the peak the polymerase stalled in a state in which the current oscillated between a dominant amplitude of ~25−28 pA for several seconds (Figure 5d). In contrast, in the presence of dATP rather than ddATP, the polymerase advanced without stalling through and beyond the 25 pA state (Figure 5e). This establishes that the stalled state observed in the presence of ddATP (which indicates replicating complexes have reached the dTMP residue) is attained *after* the template segment that causes the amplitude peak traverses the lumen. Because reaching this dTMP template residue requires the nucleotide incorporations necessary to traverse the 5ab(17,21) to 5ab(7,11) abasic configurations, these experiments verify that the characteristic amplitude peak is due to replication that ensues following ddCMP excision on the pore.

The Rate of phi29 DNAP-Catalyzed DNA Replication Is Influenced by Applied Voltage Across the Nanopore. Experiments using optical tweezers have shown that the rate of replication catalyzed by phi29 DNAP is slowed by tension on the template at forces between ~20 and ~37 pN.[26] This result predicts that the rate of phi29 DNAP replication would be influenced by the voltage applied across the nanopore. However, the voltage regime where this would occur is not known.

Figure 6 shows representative events during phi29 DNAP replication reactions along a 25 nt template segment of a DNA hairpin substrate (Figure 6a), for experiments in which the applied potential was varied in 40 mV increments in the range between 220 mV and 100 mV. The starting abasic configuration for this substrate was 5ab(25,29); therefore during DNA synthesis, the 5 abasic insert will be drawn through the limiting aperture of the nanopore lumen, spanning abasic configurations 5ab(18,22) to 5ab(6,10) and thus the amplitudes mapped in Figure 3c. These peaks were traversed at each voltage, at rates that appeared to increase as applied voltage was decreased (Figure 6b). We measured the time required to advance between two readily discernible current amplitudes corresponding to positions flanking the major current peak (blue arrows in Figure 6b, i), separated by approximately five nucleotides. At 220 mV, the median time required for replication over this distance was 227 ms (IQR = 174 ms, n = 45); at 100 mV, the median time for replication was 67 ms (IQR = 41 ms, n = 59).

Replication of Longer DNA Templates by phi29 DNAP on the Nanopore. In anticipation of replicating natural DNA templates in the nanopore, we measured phi29 DNAP-dependent replication of a longer segment within a synthetic DNA hairpin substrate. This hairpin substrate had a starting abasic configuration of 5ab(50,54), and up to 50 nucleotides can be added before the enzyme reaches the abasic block (Figure 7a). When phi29 DNAP−DNA complexes formed with this substrate were captured at 180 mV in buffer containing 0.3 M KCl, there was an initial interval of several seconds during which the current oscillated between a dominant amplitude of ~23 pA, with transitions to ~25 pA. In 27 out of 47 captured complexes that started with this oscillation, when this period ended, the polymerase proceeded to traverse the mapped amplitude peak (Figure 7b).

We speculate that this oscillating signature corresponds to complexes captured with the ddCMP terminus intact, prior to the ddCMP excision reaction that permits synthesis to ensue, because (i) a similar pattern invariably occurred between capture

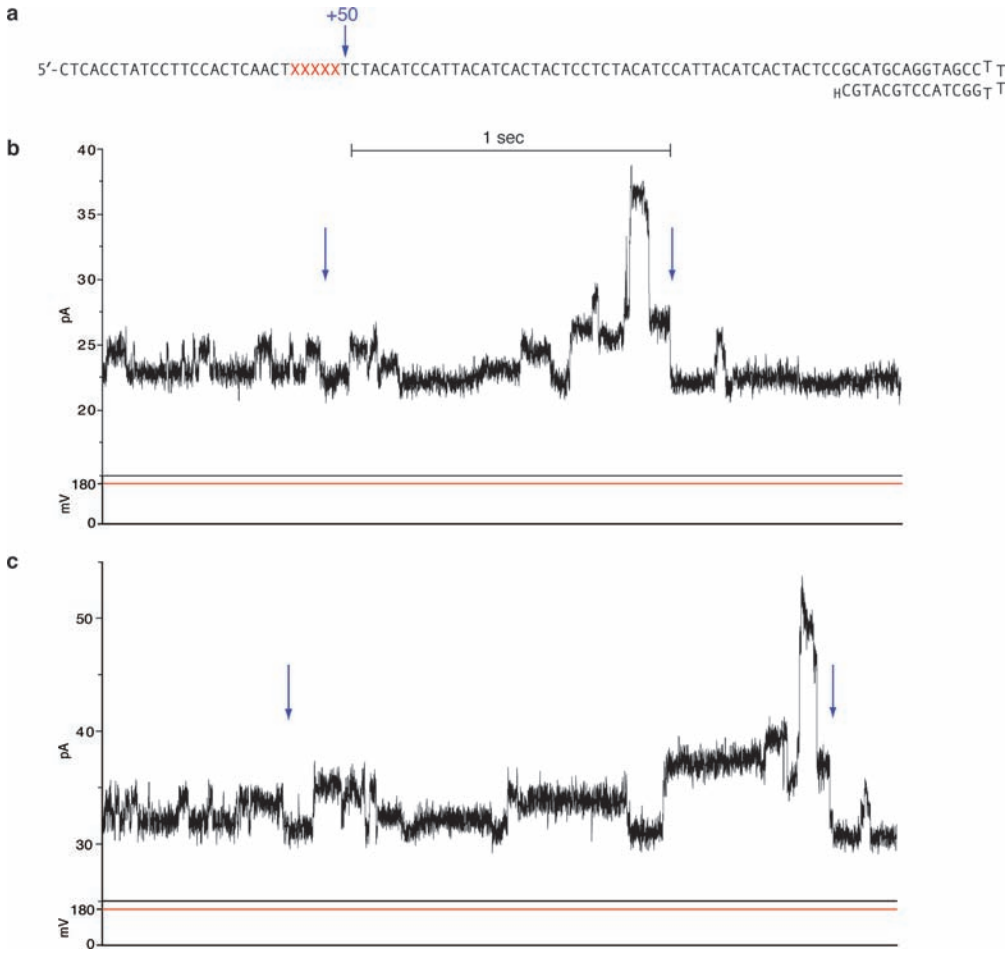

Figure 7. Processive DNA replication catalyzed by phi29 DNAP on the nanopore. (a) DNA hairpin substrate for nanopore replication experiments. The starting abasic configuration for this substrate is 5ab(50,54). After the exonucleolytic excision of the terminal ddCMP residue that is required prior to DNA synthesis, 50 nucleotides can be added before the enzyme reaches the abasic block (indicated by the blue arrow above the template strand sequence). During DNA synthesis, the 5 abasic insert is drawn toward the pore lumen as the first 32 nucleotides are incorporated and the abasic configuration 5ab(18,22) is reached; subsequent nucleotide additions then draw the block up to and past configuration 5ab(6,10). Thus, the abasic configurations in the amplitude map in Figure 3 are spanned. (b) Representative current trace at 180 mV applied potential showing phi29 DNAP replication of the hairpin substrate shown in panel a, in buffer containing 0.3 M KCl. (c) Representative current trace at 180 mV applied potential showing phi29 DNAP replication of the hairpin substrate shown in panel a, in buffer containing 0.6 M KCl. In panels b and c, the left and right blue arrows indicate the start and end points, respectively, used to approximate the time required to replicate ~50 nts along this template. Synthesis reactions were carried out in the presence of 100 μM each dGTP, dCTP, dTTP, and dATP, and were examined within the first 10 min after the addition of $MgCl_2$ to the nanopore chamber.

and synthesis for each successful replication reaction that subsequently traversed the abasic 35.4 pA peak in the experiments shown in Figures 4, 5, 6, and 7; (ii) the upper and lower amplitude levels of the oscillation differ among those experiments in a manner that depends upon the starting abasic configuration of the DNA substrate; (iii) those levels closely approximated the amplitudes for the binary and ternary complexes mapped for the abasic configuration for each substrate; and (iv) the proportion of time spent in the upper or lower amplitude state can be modulated as a function of dGTP concentration (data not shown).

We therefore used the end of this oscillating state as a starting point to approximate the time required for phi29 DNAP to traverse the ~50 nt template segment. We measured from a small but reproducible current dip that occurred just after the oscillation ended (left blue arrow in Figure 7b) to a discernible amplitude state on the distal side of the major map peak (right blue arrow in Figure 7b). The median time required to replicate across this distance in buffer containing 0.3 M KCl was 1.39 s (IQR = 0.57 s; n = 27).

Surprisingly for this mesophilic polymerase, replication of the 5ab(50,54) substrate by phi29 DNAP was also detectable in buffer containing 0.6 M KCl (Figure 7c). Like the replication reactions in 0.3 M KCl, these events began with a state in which the current oscillated between two levels for several seconds before the onset of synthesis (Figure 7c). Under these higher ionic strength conditions, the current oscillated between a dominant level of ~32 pA, with transitions to ~34 pA. Replication that drew the abasic segment through the nanopore lumen, causing the abasic block to traverse the mapped amplitude peak, ensued in 25 out of 41 events that began with this current oscillation. In 0.6 M KCl, the median time required to traverse the distance between the end of the oscillation period (left blue arrow in Figure 7c) and the distal side of the major abasic amplitude peak (right blue arrow in Figure 7c) was 2.41 s (IQR = 1.13 s; n = 25).

Discussion

The remarkable processivity and robust DNA binding properties of phi29 DNAP led us to predict that it would be a good candidate for observing processive DNA synthesis while held

atop the α-HL nanopore in an electric field. This proved to be true; phi29 DNAP−DNA complexes remained associated with the nanopore orifice and readily catalyzed sequential nucleotide additions under 180 mV applied potential. This is in sharp contrast to T7DNAP(exo-), which was difficult to retain atop the pore for sequential additions even at lower voltages.[17]

The tenacious binding of phi29 DNAP to DNA is highlighted by the different pathways by which this polymerase and KF(exo-) dissociate from DNA atop the nanopore, under conditions that do not permit exonucleolytic degradation of the DNA by phi29 DNAP. While the bond between KF and DNA can be pulled apart at 180 mV within a few milliseconds (Figure 1c) with the hairpin duplex base-pairing remaining intact,[12] dissociation from the tight binding of phi29 DNAP requires, on average, ∼20 s, and the force pulling on the template strand suspended through the pore must promote unzipping of base-pairs while the duplex is held within the confines of the enzyme (Figures 1d and 2b,c).

We exploited two features of the phi29 DNAP 3′−5′ exonuclease in this study. First, we found that a 3′-H-terminated DNA substrate was degraded more slowly in bulk phase than a 3′-OH-terminated substrate (Figure 2a). To our knowledge this is the first demonstration of discrimination against 3′-H-terminated DNA substrates by the 3′−5′ exonuclease activity of phi29 DNAP. This feature provided protection in the bulk phase against both degradation and ddNMP excision-dependent initiation of primer extension of DNA substrate molecules. This protection in turn afforded a window following the addition of Mg^{2+} to the nanopore chamber during which we could capture numerous phi29 DNAP−DNA complexes in series in which the primer terminus was intact.

Second, we used the phi29 DNAP exonuclease activity to excise the ddNMP terminus of the DNA substrate in complexes while they were held atop the pore in an electric field. In the presence of dNTPs, the polymerization reaction is highly favored over processive degradation.[30,31] Therefore, excision of the ddCMP residue to yield a primer strand 3′-OH permitted the subsequent initiation of synthesis from a defined DNA template position.

The excision of the ddNMP terminus may be accelerated in complexes by the electric field force atop the pore, as we observed that the time from complex capture to the initiation of synthesis decreased when voltage was increased (not shown). This voltage-promoted excision would nonetheless differ from the processive exonucleolytic regime induced under conditions of high template tension in optical tweezers experiments, in which processive exonucleolytic cleavage dominated even in the presence of dNTPs.[26] In contrast, while the initiation of synthesis required excision of the ddCMP residue, the polymerization reaction dominated in the nanopore experiments (Figures 4, 5, 6 and 7) even at 220 mV applied potential (Figure 6).

Maintenance of a significant pool of intact, unextended DNA substrate in the bulk phase due to the slow exonucleolytic removal of a ddNMP primer terminus allowed us to examine phi29 DNAP-catalyzed synthesis in the nanopore under relatively simple conditions. Nonetheless, due to concerns regarding the slow change in the state of the DNA molecules and potential dNTP substrate depletion in the bulk phase over time, this strategy puts constraints on the time frame in which experiments can be conducted. The use of a more robust means of protecting DNA substrate molecules in the bulk phase, such as the blocking oligomers recently employed with KF(exo-) and T7DNAP(exo-),[17] will extend the utility of this enzyme for both DNA sequencing applications and mechanistic studies of polymerase function using the nanopore.

The results of this study demonstrate that phi29 DNAP has properties ideally suited for moving long strands of DNA through nanoscale pores at a rate that is compatible with reliable base detection and identification. In this study we used only chemically synthesized DNA templates; yet the number of sequential nucleotide additions catalyzed by a single enzyme molecule that could be observed was limited only by DNA template length. Features within current traces, such as the ionic current flicker within binary complex events that can predict ternary complex amplitude (Figure 3), and the oscillation between two amplitudes upon complex capture that precedes replication reactions (Figures 4, 5, and 7), suggest that biochemical processes such as the fingers opening−closing transition[22] and dNTP binding[15] may have discernible signatures. The ability to observe dynamics in complexes under defined substrate conditions and to resolve individual catalytic cycles (Figures 4, 5, 6, and 7) in real time at high bandwidth offers the opportunity to quantify biochemical transformations as a function of applied voltage and dNTP concentration.

Acknowledgment. We thank Christopher Lam for help with nanopore mapping experiments, Ai Mai for oligonucleotide purification, Robin Abu-Shumays for comments on the manuscript, and Peter Walker (Stanford University Protein and Nucleic Acid Facility) for expert oligonucleotide synthesis. We are grateful to Christopher Benoit (Enzymatics) for supplying high specific activity, detergent-free, wild-type phi29 DNA polymerase. This work was supported by grants from NHGRI (1RC2HG005553) to M.A. and NIGMS (1R01GM087484-01A2) to K.R.L. and M.A.

Supporting Information Available: Figure S1 (sequences of 5′-6-FAM, 3′-OH and 5′-6-FAM, 3′-H DNA oligonucleotide substrates used in gel assays); Figure S2 (unbound DNA at 70 mV applied potential); Figure S3 (primer extension gel assays supporting phi2 DNAP−DNA−dGTP ternary complex formation); Figure S4 (amplitude steps in the terminal cascade vary as a function of initial DNA substrate abasic configuration); complete author list for references 4 and 5. This material is available free of charge via the Internet at http://pubs.acs.org.

JA1087612